Sensors and Actuators A 315 (2020) 112268

Contents lists available at ScienceDirect

Sensors and Actuators A: Physical

journal homepage: www.elsevier.com/locate/sna

GHz AlN-based multiple mode SAW temperature sensor fabricated on PEN substrate

Leonardo Lamanna[a,b,c,*], Francesco Rizzi[a,*], Venkat R. Bhethanabotla[c,1], Massimo De Vittorio[a,b,1]

[a] Center for Biomolecular Nanotechnologies, Istituto Italiano di Tecnologia, Via Barsanti snc, Arnesano, Italy
[b] University of Salento, Department of Innovation Engineering, Campus Ecotekne, Via Monteroni, Lecce, Italy
[c] Department of Chemical & Biomedical Engineering University of South Florida Tampa, USA

ARTICLE INFO

Article history:
Received 21 May 2020
Received in revised form 23 July 2020
Accepted 5 August 2020
Available online 27 August 2020

Keywords:
SAWs temperature sensor
Polymeric SAW devices
AlN thin film
UV microfabrication process

ABSTRACT

Polymeric based surface acoustic wave (SAW) devices represent one of the most interesting platform for the development of wireless passive sensors for IoT and smart packaging applications. An important feature to be addressed in order to develop a compact and conformable wireless SAW sensor is the increase of the working frequency which allows an easy antenna integration and miniaturization.

In this work, we present a disposable polymeric SAW temperature sensor device working in the GHz range, based on aluminum nitride (AlN) and built on a 125 μm thick film of polyethylene naphthalate. The flexible device has been compared to the same SAW device fabricated onto silicon substrates. The polymeric based SAW device shows three operating wave modes corresponding to the Rayleigh, Love, and Lamb, highlighting that the Lamb mode exhibits a resonance frequency as high as 1.325 GHz, corresponding to a phase wave velocity of 10,600 m/s, an electromechanical coupling of 2.91 % and Q factor of 109. Temperature coefficient of frequency (TCF) values of 149, 109, 53 ppm/°C have been calculated for the Rayleigh, Love and Lamb waves, respectively.

The different behavior of the three SAW modes let us envision the development of a multiple sensing platforms based on different modes in the same device (*e.g.* temperature, microbiological contamination, light exposure).

1. Introduction

Over the last decades Radio Frequency Identification (RFID) has found application in different fields such as inventory tracking and management, retail level management, access control, animal tracking, security and electronic toll collection [1]. At the age of the Internet of Thing (IoT), the RFID-enabled temperature sensors will expand their applications in the cold-chain logistics (*e.g.* food and pharmaceuticals) both in storage and transportation. Analogously, they can be applied in control of many medical diagnostic tests and procedures (*e.g.* supplies of plasma, biological reagent) [2].

Surface acoustic wave (SAW) -based RFID is one of the most promising technology in this field, taking advantage of being a passive wireless sensor technology, with respect to the common sensor integrated with the RFID [3,4]. In this regard, research on SAW sensors continue to advance, demonstrating the possibility of label-free biosensors [5], sensors for environmental particulate monitoring [6], sensors for quality control [7–9] and SAW light detectors [10,11]. Moreover, SAW based device intrinsically owns temperature sensing capability since SAW propagation velocity is affected by the temperature [12]. In literature, many SAW-based temperature sensors are reported. Usually, these devices are fabricated on thick piezoelectric materials or on thin piezoelectric film deposited on silicon. Recently, improvement in the sputtering deposition has allowed the development of SAW device on inexpensive soft polymeric substrates [8,11–13]. The exploitation of conformable, inexpensive and recyclable device is one fundamental step to drive this technology to large scale monitoring application [8]. In order to develop such a SAW-RFID sensor a design of a high frequency working device must be implemented, allowing an easy antenna integration and miniaturization. In particular, the GHz range in industrial, scientific, and medical (ISM) frequencies,

* Corresponding author at: Center for Biomolecular Nanotechnologies, Istituto Italiano di Tecnologia, Via Barsanti snc, Arnesano, Italy.
E-mail addresses: leonardo.lamanna@iit.it (L. Lamanna), francesco.rizzi@iit.it (F. Rizzi).
[1] These authors jointly supervised this work.

https://doi.org/10.1016/j.sna.2020.112268
0924-4247/

includes a number of bands that can be used without licensing when using a limited radiated power [3,14].

The development of aluminum nitride (AlN) based acoustic devices is the most promising technology to obtain a RFID SAW sensors due to its high acoustic velocity among piezoelectric materials [15]. In an acoustic device, the application of radiofrequency (RF) signal to the metallic electrodes allows the generation and propagation of acoustic waves along the piezoelectric material. The center frequency of these devices is given by $f_0 = v_A/\lambda$ where the velocity v_A depends on the substrate's mechanical properties and the type of the traveling wave, while the wavelength λ depends on the distance between the electrodes. Acoustic devices based on thin piezoelectric film are divided in two main classes: film bulk acoustic resonator (FBAR) and surface acoustic wave (SAW) devices. In the FBAR the thickness of piezoelectric layer determines wavelength and operating frequency of the FBARs, which ranges from sub-GHz to tens of GHz [13,16]. Such devices are the optimal candidate for high-frequency devices [17], but they present many disadvantages: fragility, due to their membrane-based structures, more complicated fabrication and high noise to signal ratio. Instead, SAW devices present the advantage of an easy microfabrication process, sensing and actuator capability and integrability in Lab on a Chip technology, but, usually, they present a lower working frequency [13].

SAWs devices based on c-axis (0002) oriented AlN allow two principal wave propagation modes: Rayleigh waves (R-SAWs) and Lamb waves (L-SAWs). The R-SAWs are favored in the AlN grown on rigid substrates (usually silicon) and propagate at a phase velocity of about 5000 m/s; instead, the L-SAWs are favored in membranes and when grown on polymeric soft substrates, travel at a phase velocity of about 10,000 m/s [12,13].

Nowadays, the limitation in the development of R-SAW devices at high frequency is principally due to the use of expensive substrates such as diamond (that slightly increases the phase velocity) and limitations in the microfabrication process [18]. In fact, to achieve GHz working frequency devices, it is necessary to utilize expensive and time consuming fabrication processes, such as electron-beam lithography, to reduce the IDTs dimension and SAW wavelength [19,20]. At the same time, L-SAWs allow a higher frequency, due to their intrinsic higher phase velocity, making possible to exploit UV photolithographic processes to obtain GHz SAW devices. Nevertheless, this latter L-SAWs based device has not been widely reported, due to the difficult fabrication of thin fragile AlN suspended membrane or challenging growth of piezoelectric AlN thin layers on polymeric substrate [13,20]. Recent improvements of the sputter deposition technique allowed the growth of AlN at low temperature with high c-axis (0002) orientation, enabling the deposition on a few polymeric substrates such as polyimide [21] and polyethylene naphthalate [12]. The use of these substrates is paving the way to an easier exploitation of the L-SAWs on AlN, reducing the problems of membrane fabrication and fragility, enabling the development of a new class of polymeric, conformable and high frequency SAW sensors devices [8,10]. Although in the lasts years, polymeric SAW devices have been explored for sensing UV, strain, pressure, humidity, temperature, and bacteria [8,10,11,13,22,23], no SAW sensor in the GHz range has been demonstrated so far.

In this work, the development of the first polymeric based SAW temperature sensor working in the GHz range is demonstrated. The fabrication of a Polyethylene Naphthalate (PEN) /AlN based SAW devices [8,12] by bilayer lift-off photo-lithography optimized for aluminum IDTs on polymeric PEN substrate allowed us to preserve a low surface roughness of the sputtered AlN, which is irreparably damaged when exploiting dry or wet aluminum etching processing. The lift off process led to a surface preservation, improving the SAWs propagation at higher frequency. Finally, the use of aluminum as IDTs metal increases the surface acoustic energy confinement [13] obtaining a transmission signal amplitude up to 20 dB at 1.325 GHz with IDTs size and resolution in the micrometric range. The developed devices were applied to the fabrication of the first conformable polymeric temperature sensor working with a the Rayleigh, Love and Lamb multimode SAWs and showing temperature coefficients of frequency (TCF) of 149, 109, 53 ppm/°C, respectively.

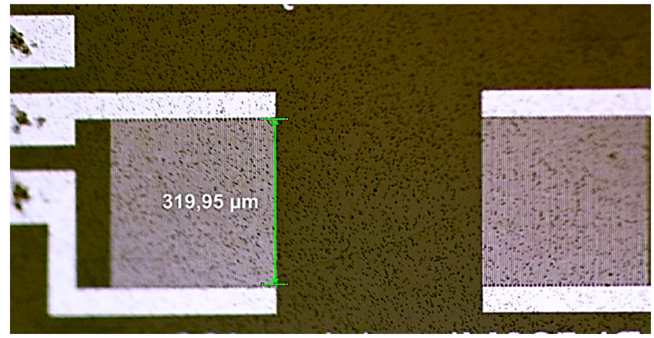

Fig. 1. optical micrograph of fabricated devices with detail on the acoustic aperture.

2. Design

SAW delay line sensors are obtained by fabricating two metallic interdigital transducers (IDT) on the piezoelectric film, whose purpose is the transmission (input IDT) and detection (output IDT) of a SAW. The generation of a time dependent piezoelectric deformation due to the application of an AC signal leads to the generation of the traveling waves.

As mentioned above, in order to obtain a higher frequency SAW sensors, a lift-off process for an IDT pitch size scale down is needed. A wavelength of 8 µm needs a 2 µm wide finger, representing on polymeric based substrate a technological challenge for lift-off UV photolithography [24]. In fact, the photoresist processing for a lift-off process on a soft polymeric substrate, as well-known, presents many challenges due mainly to poor resist adhesion and consequent non uniform spin coating, and difficult baking temperature control [24]. In this contribution, a bilayer lift-off processing has been optimized in order to deposit 100 nm aluminum and define a polymeric based SAW device with 2 µm fingers. To the best of our knowledge this is the smallest structure exploited for the development of a polymeric based SAW devices working in the GHz range. The SAW delay line fabricated (fig. 1) consists in 2 identical IDTs with 40 pairs of fingers with λ = 8 µm and metallization ratio of 0.5 (finger 2 µm) made of 100 nm aluminum. The device presents an aperture of 320 µm and a delay line of 50 λ. Three pads of 150 µm for a coplanar probe coupling have been designed.

3. Microfabrication

The bilayer lift-off process starts with spin coating of a non-photosensitive material (LOR-10B, MicroChem) followed by a second layer of AZ1512 (MicroChemicals GmbH) photoresist. Usually, such bilayer resist is stripped by metal-ion-free (MIF) or a sodium-based buffer developer, both etching aluminum and AlN. In our case, to pattern a 100 nm thick aluminum layer, we have used the REMOVER 1165 (Microposit), which does not etch the aluminum-based materials. SAW delay line devices have been fabricated on two different substrates: rigid silicon and flexible PEN, to compare the wave propagation of R-SAWs and L-SAWs, respectively. The AlN deposition process has been described and characterized in our previous publication [12] and will be briefly outlined here.

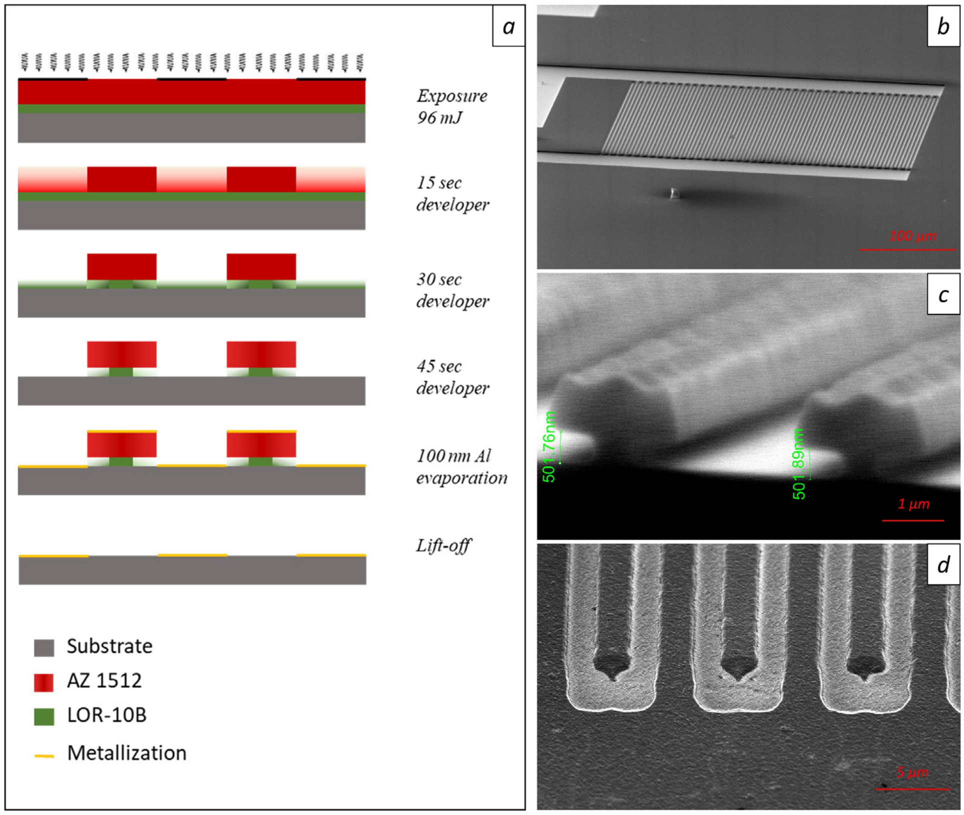

Fig. 2. a) Metal lift-off process sequence utilizing bilayer technique; b,c) Bi-layer resist pattern SEM micrograph of: a complete IDT and a fingers cross-section, respectively, resulting from the process flow given Table 1;d) SEM micrograph after lift-off of a 100-nm-thick aluminum. All the pictures have been acquired with a tilt angle of 42°, 30 kV and $2.27e^{-1}$ Torr.

High frequency AlN based SAW sensors were fabricated on 125 µm thick PEN, purchased from Teonex (code Q65HA) with one pretreated surface which improves the growth adhesion [25]. The PEN sheets (3 × 3 cm) were fixed on a silicon substrate, by a removable PDMS layer, in order to allow a uniform deposition and reduce the temperature stress which occurs during the AlN deposition. Multistep AlN sputtering growth technique, each step for depositing 1.5 µm thick AlN, has been performed to deposit 4.5 µm of piezoelectric AlN on PEN substrate to be exploited for the fabrication of a polymeric-based SAW device. Such sputtering deposition, optimized in the last years by our group on different polymeric substrate [12,21,26,27], allows the growth of piezoelectric AlN layer keeping as low as possible (< 180 °C) the temperature in the chamber, avoiding the generation of lattice stress and cracks generation. The growth shows high C-axis crystal orientation with an average grain size of 50 nm, surface roughness of approximately 7.5 nm and effective piezoelectric coefficient of 3.3 pm/V. The same characterization results have been obtained on silicon; both substrates were utilized for SAW device fabrication [8,11,12].

As shown in Fig. 2a the exploitation of a bilayer lift off technique facilitates the generation of a shadow area generated by the underetching of the first layer, enabling metal deposition without defects.

The key point in design of this process for IDTs fabrication is the aspect ratio between the photoresist finger mask thickness and the first nonphotosensitive layer thickness that must be larger than two. In our case, for the generation of 2 µm finger with metallization of 100 nm, the thickness of the first layer ideally should be in a range between 200 nm (limitation given by the metallization) and 800 nm (limitation given by the underetching). Therefore, it became necessary to set a LOR-10B / G Thinner (MicroChem) dilution ratio equal to 1:3 in order to have a viscosity reduction enough to reduce the spin coated nonphotosensitive first layer thickness. Therefore, the thickness reduction of the first layer allowed a controllable underetching during the isotropic development process carried out by AZ 726 MIF.

Fig. 2b,c show scanning electron microscopy (SEM) of complete IDT and a fingers cross-section of the developed bilayer microfabrication process, respectively. Fig. 2c shows that the first nonphotosensitive layer is thick around 500 nm and the structures are thick around 1500 nm with evidence of the T-profile structure, necessary for a lift-off process. Our process has proved to be reproducible, compatible with rigid and soft polymeric substrates and with a wide range of metal compatible with REMOVER 1165 (up to 500 nm thick). After the conclusion of the developing process, devices were oxygen plasma treated to clean up any leftover resist and allow optimum metal adhesion. Finally, 100 nm thick aluminum layer (99.95 % pure) was deposited using a Varian e-beam evaporator and successfully lifted off (Fig. 2d). Deposition of 100 nm of Al does not introduce any relevant stress to the device, indeed, the e-beam evaporation allows a low-temperature deposition.

4. Results and discussion

The fabricated devices were preliminarily electrically characterized using a vector network analyzer (Agilent 8753ES) at room temperature using a |Z| Probe with 150 µm pitch. All the data in the paper refer to three identical devices from three different production batches, noteworthy, all the spectra were acquired 50 times and averaged by the Agilent 8753ES. Fig. 3 shows the transfer functions S_{21}, obtained by the measurements of the delay lines on both substrates. The values of the out-of-band insertion loss ranging between -60/-70 dB for the silicon substrate and -70/-80 dB in the devices fabricated on PEN, proving low feedthrough between

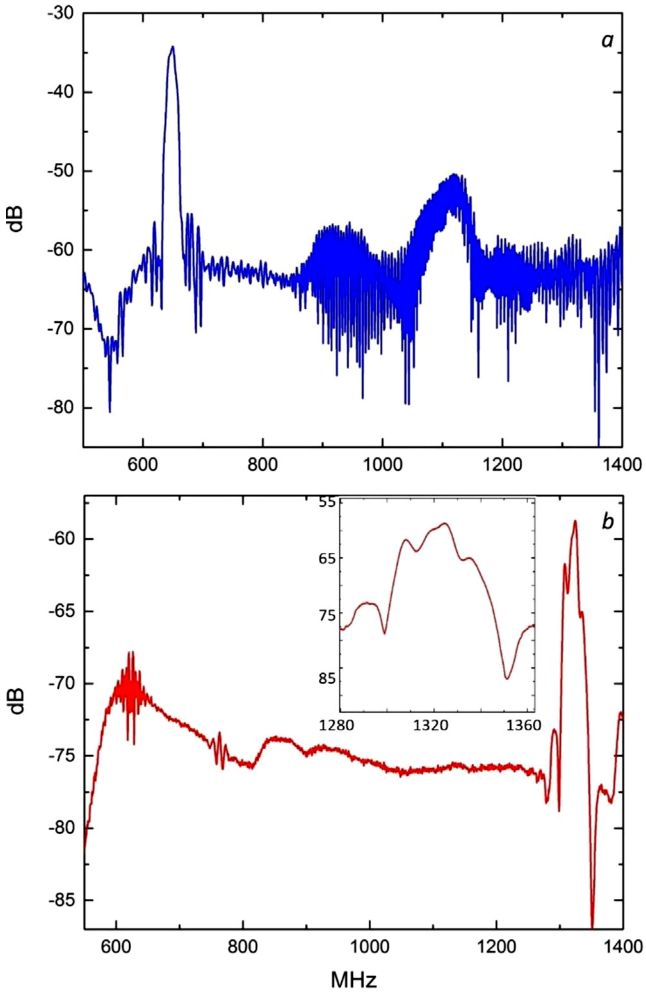

Fig. 3. a,b) Transfer function amplitude S_{21} of the devices fabricated on rigid silicon and PEN substrates, respectively; inset in the figure b shows a zoom of the Lamb wave resonance.

the interdigital transducers (IDTs) [28]. Due to the impedance mismatch of the device, both samples show a non-negligible in-band insertion loss.

The analysis of the transfer functions on a silicon substrate (Fig. 3a) shows the propagation of one SAW mode corresponding to the Rayleigh wave. The R-SAWs propagation highlights a *Sinc* function as expected for uniform IDT SAW devices [29]. The center frequency is around 650 MHz corresponding to the SAW phase velocity of 5200 m/s. Noteworthy, in the silicon substrate a series of spurious signal in S_{21} are reported in the range between 850–1200 MHz. Such signals, as Zhou et al. reports, are attributed to a multiple reflection of wave generated at the input IDT on the AlN/silicon interface in nonideal situation, or to resonances and multiple reflections at the various interfaces, and detected at the output IDT [30,31].

On the other hand, on PEN polymeric substrate, two SAWs modes are mainly showed, corresponding to Rayleigh waves at lower frequency and Lamb waves at higher frequency. There are peculiar differences in the propagation of the two modes: while the Rayleigh waves show spurious signals with a central resonance frequency at 620 MHz (corresponding to a phase velocity of 4960 m/s), the Lamb waves exhibit a *Sinc* function signal with a central resonance frequency at 1.325 GHz corresponding to a phase velocity of 10,600 m/s). The different behavior between the two substrate originates from their different mechanical properties. In

Table 1
Microfabrication process flow recipe.

Process step	Comment
Sample cleaning	Acetone /isopropanol/water
Drying	10 min at 100 °C
Spin coating of non-photosensitive material	Spin LOR-10B : G Thinner (1:3) for 40 s at 4500 rpm
Bake	180 °C 5min
Spin coating of a photosensitive material	Spin AZ 1512 for 40 s at 2500 rpm
Bake	50 s at 110 °C
Exposure hard contact	405 nm 96mJ
Post bake	2 min 110 °C
Develop	AZ 726 MIF developer 45–50 s
Oxygen plasma cleaning	1 min
Aluminum evaporation	Electron-beam physical vapor deposition of 100 nm of aluminum 99.95 %
Lift off in REMOVER 1165	1h at 75 °C

Table 2
Material properties used in the FEM modeling.

Material	Density (Kg/m^3)	Young modulus (GPa)	Poisson ratio
Aluminum	2700	70	0.33
PEN	1360	12.2	0.49
AlN	3300	340	0.25

particular, R-SAWs, that are transversal waves traveling on the surface, are favored in bulk materials and in thin films grown on a rigid substrate; L-SAWs, instead, are waves that travel within the piezoelectric layer, favored in piezoelectric membranes and thin films grown on polymeric substrates. Moreover, the transmission spectra on the polymeric substrate showed dips near the central frequency of the lamb resonance (Fig. 3b). Incoherent resonance by individual IDT fingers is responsible for the dips, which are due to the acoustic waves that penetrate into the polymer substrate generating incoherence because of the high mechanical mismatch between AlN and PEN [32]. Noteworthy, in the PEN based SAW devices, a third minor signal at 763 MHz is shown. This mode corresponds to shear horizontal/Love wave (SH) propagation: in fact, such frequency matches a phase wave velocity of 6106 m/s in accordance with the SH-SAWs velocity on AlN [33,34].

To verify the different SAW propagation modes, a series of 3D finite element model (FEM) simulations were carried out. The model used in the previous work [12], describing the SAW elemental cell, has been implemented with new material parameters and geometry, to find the superficial wave eigenmodes. Table 2 describe the main material data used in the FEM model.

Fig. 4 shows the superficial SAW eigenmodes on a PEN substrate; Rayleigh (Fig. 4a), Love (Fig. 4b) and Lamb (Fig. 4c) waves at 613, 760 1388 MHz, respectively, are identified. Simulated frequencies are very close to the measured resonance frequencies, with an average deviation of 1%, confirming the nature of the SAWs at the different frequencies ().

Rayleigh and Lamb waves resonances, on silicon and PEN substrate respectively, have shown a large transmission signal amplitude, up to 20 dB, indicating that the out-of-band/in-band power ratio is 0.01, showing a remarkable signal to noise ratio. The reduction of the wavelength and the improvement in the microfabrication, with the exploitation of bilayer lift off process, enhances the signal-to-noise ratio allowing the detection of the Love wave usually not favored on c-axis oriented AlN-based SAW devices [13].

The electromechanical coupling K^2, has been estimated exploiting the equivalent circuit model of SAW IDT using S_{11} scattering parameter method [34,35]. Assuming IDT equivalent circuit as a parallel between its intrinsic and parasitic parts, a model can be setup. Briefly, the intrinsic part consists of the total capacitance of

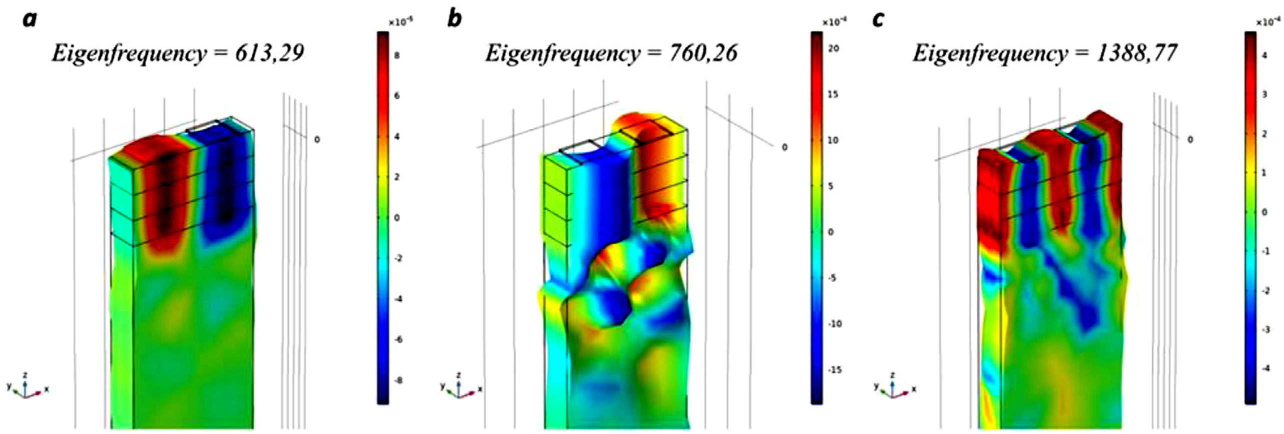

Fig. 4. FEM simulation: a,b,c) superficial eigenfrequency for a triple layer of AlN on PEN substrates corresponding to the Rayleigh, Shear and Lamb wave propagation, respectively.

the IDT, its radiation conductance, and the radiation susceptance; the parasitic part, instead, consists of the parasitic capacitance and the parasitic conductivity [36]. The applied formula is:

$$K^2 = \frac{G}{8 N f_0 C_i} \quad (1)$$

where G is the experimental conductance at the resonance frequency (0.16 and 0.147 MΩ for silicon and PEN, respectively), N is the number of finger pairs, f_0 is the central resonance frequency, C_i is the input capacitance at f_0 and is determined by the measured susceptance (B) through the relationship ($C_i = B/(2\pi f_0)$) (0.13 and 0.099 MΩ for silicon and PEN, respectively) [12,35,37]. The electromechanical coupling, calculated for the R-SAWs on silicon and L-SAWs on PEN polymeric substrate are 2.61 % and 2.91 %, respectively. Noteworthy, the measured coupling is higher than previously reported K^2 on polymeric based SAW devices [22,32,38]. Moreover, the experimental Q factor has been determined using the -3 dB method:

$$Q = \frac{f_0}{\Delta f_{-3dB}} \quad (2)$$

Where Δf_{-3dB} is the bandwidth at -3 dB. A Q factor of 52 and 109 have been calculated for Rayleigh on silicon and Lamb on PEN, respectively [13]. The higher Q for the Lamb wave on the polymeric substrate indicates a lower rate of energy loss, with the oscillations dying out more slowly [39]. The electrical characterization results confirm the expected higher AlN/Al performance in the SAW device, in respect with other materials combination, for both electromechanical coupling and Q factor [13], envisioning an application in the RFID sensor system.

5. Temperature sensing

SAW devices, thanks to their sensitivity, reliability and wireless capability, are widely exploited for the realization of various types of sensors. For instance, mass loading based SAW sensor have shown higher sensitivity for biomarker compared to electrochemical ones [8,9,32]. Wireless SAW sensors have been employed to monitor external physical environment parameters (*e.g.* temperature, pressure) [40–42]. High frequency polymeric conformable SAW sensors can play an important role in this respect thanks to cost reduction and compliance, making these devices widespread in industrial and logistic applications [8]. In this work the developed GHz polymeric-based SAW devices have been tested to evaluate the suitability for the realization of the first SAW RFID temperature sensor.

The thermal frequency sensitivity of resonators is characterized by the temperature coefficient of frequency (TCF), defined as the change of the resonance frequency with the temperature;

$$TCF = \frac{df}{f_0\, dT} \quad (3)$$

it is usually expressed as ppm/°C. It is well known that the velocity and amplitude of the acoustic wave depend on various physical parameters such as temperature and pressure. In particular, a decreasing of the resonance frequency is typically reported with the temperature increasing [40,42,43]. Such shift of the resonance frequency is due to different parameters and mainly related to the temperature coefficient of expansion (TCE) of the employed materials [13].

In this work, the devices have been tested at different temperatures in a range between 20 and 120 °C with a step of 20 °C, with the experimental set up shown in fig.5a. The resonance frequency variation (fig.5b) has been calculated exploiting a cross-correlation algorithm between transfer function spectra at different temperatures. For the Rayleigh wave on silicon substrate (green line) and for the Rayleigh, Love and Lamb wave for the PEN substrate (gray, red, and blue lines, respectively). A TCF value of 64 ppm/°C has been calculated for the R-SAW on the silicon substrate instead a TCF values of 149, 109, 53 ppm/°C for the Rayleigh, Love and Lamb wave, respectively, have been calculated for devices fabricated on PEN. The higher TCF of the Rayleigh and Love waves, with respect to the Lamb mode in the PEN substrate, is due to the diverse waves properties. The Lamb waves travel within the piezoelectric layer and are less affected by the substrate mechanical properties variation due to the temperature increasing. In contrast, the Rayleigh and Love modes travel in both piezoelectric and substrate, in which the deformation decays with the thickness. Therefore, such modes are more affected by the substrate thermal changes. At higher frequencies (with a lower λ/h ratio, h is the piezoelectric layer thickness), most of the deformation of Rayleigh and Love waves falls in the piezoelectric layer with a minor influence of the substrate. In fact, compared to a previously reported value for lower frequencies [12], we have measured a smaller TCF for the Rayleigh wave on the PEN substrate. Fig. 5b shows a larger error bars related to the Rayleigh waves on polymeric substrate which could be attributed to a double effect: *i)* since the Rayleigh waves on polymeric substrate are highly sensitive to the AlN thickness, small variation in the AlN deposition could generate fluctuation in the temperature sensitivity (the data are referred to devices from three production batches); *ii)* the spurious signals related to the Rayleigh modes do not allow a precise identification of the resonance frequencies. In contrast,

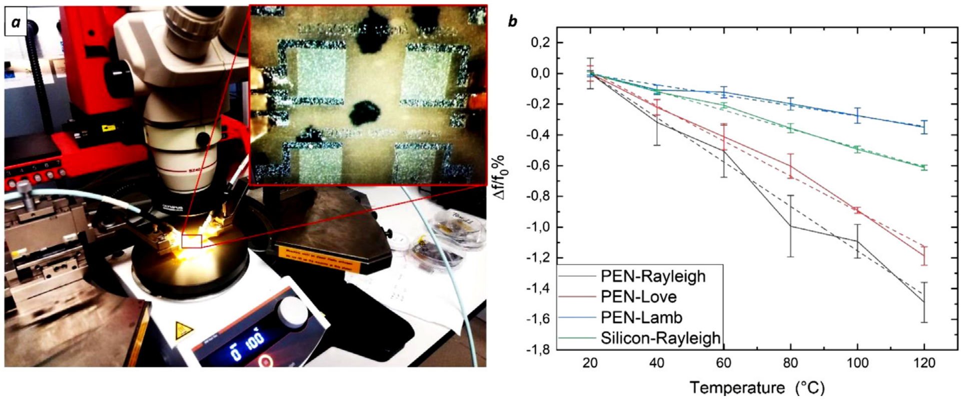

Fig. 5. a) Experimental setup used for the temperature stability characterization, the inset shows the view of the optical microscope from the top; b) show the normalized resonant frequency shift as a function of temperature.

the symmetric Lamb SAWs in AlN are waves that travel within the piezoelectric layer and are less influenced by the AlN layer thickness and PEN substrate [12,13]. Better understanding of the correlation between the TCF and the piezoelectric layer thickness and properties is indicated as future research.

The temperature responsivity, in the analyzed range, could be also linearly approximated and calculated as *df/dT*. Responsivity of 93.4 kHz/°C (R^2 of 0.98), 89.8 kHz/°C (R^2 of 0.99), and 46.9 kHz/°C (R^2 of 0.98) have been obtained for the Rayleigh Love and Lamb wave on the PEN substrate, respectively, and 39.5 kHz/°C (R^2 of 0.98) for the Rayleigh wave on silicon. Moreover, the Limit of Temperature Detection (LoTD) has been calculated for all the modes, across different batches, within a 95 % confidence interval, according to Armbruster et al. [44] using the data of the three different batches. A LoTD equals to 11, 5 and 6 °C are calculated for Rayleigh, Love and Lamb waves on PEN, respectively, while, a LoTD of 4 °C has been calculated for the Rayleigh wave on Silicon substrates. The reason for these higher LoTD values, with respect to the ones reported in the literature, is mainly due to the calculation across differences production batches with fluctuation in the AlN thickness which generates variability in the temperature sensing. However, in spite of having a LoTD in the range of a few °C, the development of these polymer-based SAW devices thanks to their conformability, recyclability and cost reduction will pave the way to the development of inexpensive SAW-RFID temperature sensors relevant for application such as smart packaging of food, pharmaceutical or in general in the cold chain, where the required temperature performance are coarse.

L-SAWs based temperature sensor, in spite of the lower TCF and higher LoTD, has shown highly reproducibility among different batches. Moreover, the better electrical properties (*e.g.* large transmission signal amplitude and high electromechanical coupling) let us envision an easier application as RFID transducer, being this, to the best of our knowledge, the first polymeric SAW temperature sensor working in the GHz range.

6. Conclusion

In summary, this work presents the first polymeric based GHz SAW temperature sensor device fabricated by exploiting an optimized bilayer aluminum lift-off process. The increasing of the working frequency is an important step forward to develop a proper polymeric RFID SAW sensor, allowing an easy antenna integration and miniaturization. Three different modes have been reported on the polymeric substrate corresponding to the Rayleigh, Love and Lamb waves, in good agreement with FEM simulations. A frequency as high as 1.325 GHz with K^2 of 2.91 % and Q factor of 109 has been achieved on the polyethylene naphthalate 125 μm film. The frequency corresponds to a wave phase velocity of 10,600 m/s, exploiting the Lamb wave propagation on such polymeric substrate. The device highlights a large transmission signal amplitude up to 20 dB at such frequency, important feature for RFID realization. The devices have been exploited as a multiple mode temperature sensor reporting TCF values of 149, 109 and 53 ppm/°C for the Rayleigh, Love and Lamb wave on PEN substrate, respectively. The use of soft polymeric substrates is paving the way for easier exploitation of the high phase velocity of Lamb SAWs on AlN, reducing the problems of membrane fabrication and fragility, with the advantage of high-frequency devices easily integrable with RFID systems and applicable in the smart food packaging. Moreover, the different behavior for Rayleigh, Love and Lamb waves could be exploited in multiple sensing platforms based on different modes in the same device (*e.g.*, temperature, bacterial contamination, light exposure, etc...) useful in the food chain control.

Author contributions

L.L., F.R., V.R.B. and M.D.V. designed the work. L.L. growth piezoelectric material, fabricated the devices and carried out the device performance characterization. L.L. and F.R. performed the model simulation based on FEM COMSOL and analytical calculations. L.L. wrote the manuscript, with input from all authors.

Declaration of Competing Interest

The authors declare no competing interests.

Acknowledgments

This work was partially funded by the National Science Foundation (Grant No. IIP-1640668), which is gratefully acknowledged.

Appendix A. Supplementary data

Supplementary material related to this article can be found, in the online version, at https://doi.org/10.1016/j.sna.2020.112268.

References

[1] A. Rida, et al., Development and implementation of novel UHF paper-based RFID designs for anti-counterfeiting and security applications, in: 2007 International Workshop on Anti-Counterfeiting, Security and Identification (ASID), IEEE, 2007.
[2] A. Kang, et al., SAW-RFID enabled temperature sensor, Sens. Actuators A Phys. 201 (2013) 105–113.

[3] V.P. Plessky, L.M. Reindl, Review on SAW RFID tags, IEEE Trans. Ultrason. Ferroelectr. Freq. Control 57 (3) (2010) 654–668.
[4] I. Marasco, et al., Compact and flexible meander antenna for surface acoustic wave sensors, Microelectron. Eng. (2020) 111322.
[5] K. Chang, et al., Label-free and high-sensitive detection of human breast cancer cells by aptamer-based leaky surface acoustic wave biosensor array, Biosens. Bioelectron. 60 (2014) 318–324.
[6] M.S. Chiriacò, et al., Optimization of SAW and EIS sensors suitable for environmental particulate monitoring, Microelectron. Eng. 202 (2018) 31–36.
[7] H. Yao, et al., A Surface Acoustic Wave (SAW) biosensor method for functional quantification of E. Coli L-asparaginase, Talanta 203 (2019) 9–15.
[8] L. Lamanna, et al., Conformable surface acoustic wave biosensor for E-coli fabricated on PEN plastic film, Biosens. Bioelectron. (2020) 112164.
[9] M. Agostini, G. Greco, M. Cecchini, A rayleigh surface acoustic wave (r-SAW) resonator biosensor based on positive and negative reflectors with sub-nanomolar limit of detection, Sens. Actuators B Chem. 254 (2018) 1–7.
[10] L. Lamanna, et al., Photoresponse of the AlN-based SAW device on polymeric and silicon substrates, IEEE Sens. J. (2020) 1.
[11] L. Lamanna, et al., Light interaction with AlN-based SAW device fabricated on flexible and silicon substrate, in: 2019 IEEE SENSORS, IEEE, 2019.
[12] L. Lamanna, et al., Flexible and transparent aluminum-nitride-Based surface-acoustic-Wave device on polymeric polyethylene naphthalate, Adv. Electron. Mater. (2019) 1900095.
[13] Y.Q. Fu, et al., Advances in piezoelectric thin films for acoustic biosensors, acoustofluidics and lab-on-chip applications, Prog. Mater. Sci. 89 (2017) 31–91.
[14] A. Pohl, A review of wireless SAW sensors, IEEE Trans. Ultrason. Ferroelectr. Freq. Control 47 (2) (2000) 317–332.
[15] J. Meinschien, et al., Smooth and oriented AlN thin films deposited by laser ablation and their application for SAW devices, Appl. Phys. A 69 (1) (1999) S683–S686.
[16] Y. Jiang, et al., A flexible, gigahertz, and free-standing thin film piezoelectric MEMS resonator with high figure of merit, Appl. Phys. Lett. 111 (2) (2017) 023505.
[17] C. Zhou, et al., Flexible structured high-frequency film bulk acoustic resonator for flexible wireless electronics, J. Micromechanics Microengineering 25 (5) (2015) 055003.
[18] J. Rodriguez-Madrid, et al., Super-high-frequency SAW resonators on AlN/diamond, IEEE Electron Device Lett. 33 (4) (2012) 495–497.
[19] P. Kirsch, et al., 5 GHz surface acoustic wave devices based on aluminum nitride/diamond layered structure realized using electron beam lithography, Appl. Phys. Lett. 88 (22) (2006) 223504.
[20] J. Bjurström, I. Katardjiev, V. Yantchev, Lateral-field-excited thin-film Lamb wave resonator, Appl. Phys. Lett. 86 (15) (2005) 154103.
[21] F. Guido, et al., AlN-based flexible piezoelectric skin for energy harvesting from human motion, Microelectron. Eng. 159 (2016) 174–178.
[22] X. He, et al., High sensitivity humidity sensors using flexible surface acoustic wave devices made on nanocrystalline ZnO/polyimide substrates, J. Mater. Chem. C 1 (39) (2013) 6210–6215.
[23] W. Xuan, et al., Flexible surface acoustic wave humidity sensor with on chip temperature compensation, Procedia Eng. 120 (2015) 364–367.
[24] Z. Cui, Nanofabrication, in: Course Notes, ECE, 2008, pp. 730.
[25] Teonex®. Teonex® PEN film Technical Information. Available from: https://www.cmc-klebeband.de/media/files/Teonex–PEN-Technical-Brochure.pdf.
[26] V.M. Mastronardi, et al., Low stiffness tactile transducers based on AlN thin film and polyimide, Appl. Phys. Lett. 106 (16) (2015) 162901.
[27] S. Petroni, et al., Flexible piezoelectric cantilevers fabricated on polyimide substrate, Microelectron. Eng. 98 (2012) 603–606.
[28] M. Clement, et al., SAW characteristics of AlN films sputtered on silicon substrates, Ultrasonics 42 (1-9) (2004) 403–407.
[29] C. Campbell, Surface Acoustic Wave Devices for Mobile and Wireless Communications, Four-Volume Set, Academic press, 1998.
[30] J. Zhou, et al., Discrete microfluidics based on aluminum nitride surface acoustic wave devices, Microfluid. Nanofluidics 18 (4) (2015) 537–548.
[31] F. Marshall, New technique for the suppression of triple-transit signals in surface-acoustic-wave delay lines, Electron. Lett. 8 (12) (1972) 311–312.
[32] H. Jin, et al., Flexible surface acoustic wave resonators built on disposable plastic film for electronics and lab-on-a-chip applications, Sci. Rep. 3 (2013) 2140.
[33] J. Xu, et al., Propagation of a shear-horizontal surface acoustic mode in a periodically grooved AlN/Al 2 O 3 microstructure, J. Appl. Phys. 96 (1) (2004) 212–217.
[34] A. Wright, Elastic properties of zinc-blende and wurtzite AlN, GaN, and InN, J. Appl. Phys. 82 (6) (1997) 2833–2839.
[35] N. Shigekawa, et al., Side-gate effects on transfer characteristics in GaN-based transversal filters, Appl. Phys. Lett. 87 (8) (2005) 084102.
[36] W.R. Smith, et al., Analysis of interdigital surface wave transducers by use of an equivalent circuit model, IEEE Trans. Microw. Theory Tech. 17 (11) (1969) 856–864.
[37] L. Shu, et al., The characterization of surface acoustic wave devices based on AlN-metal structures, Sensors 16 (4) (2016) 526.
[38] X. He, et al., High performance dual-wave mode flexible surface acoustic wave resonators for UV light sensing, J. Micromech. Microeng. 24 (5) (2014) 055014.
[39] R. Abdolvand, H. Fatemi, S. Moradian, Quality factor and coupling in piezoelectric mems resonators, in: Piezoelectric MEMS Resonators, Springer, 2017, pp. 133–152.
[40] R. Fachberger, A. Erlacher, Applications of wireless SAW sensing in the steel industry, Procedia Eng. 5 (2010) 224–227.
[41] K. Lee, et al., A novel 440 MHz wireless SAW microsensor integrated with pressure–temperature sensors and ID tag, J. Micromech. Microeng. 17 (3) (2007) 515.
[42] H. Oh, et al., Sensitivity improvement of wireless pressure sensor by incorporating a SAW reflective delay line, Int. J. Smart Sens. Intell. Syst 1 (4) (2008) 940–954.
[43] P.K. Das, A.D. Snider, V.R. Bhethanabotla, Acoustothermal heating in surface acoustic wave driven microchannel flow, Phys. Fluids 31 (10) (2019) 106106.
[44] D.A. Armbruster, T. Pry, Limit of blank, limit of detection and limit of quantitation, Clin. Biochem. Rev. 29 (Suppl 1) (2008) S49.

Biographies

Leonardo Lamanna currently is a fellow at the IIT. He got BS in *Biotechnology* and MS in *Nanobiotechnology*. Afterward, he was employed in the R&D department of the biomedical company "Gelesis Inc.". His job was focused on the hydrogel synthesis and characterization, and evaluation of drug-device interaction. He left the job for a PhD position in *Engineering of materials and nanotechnology* at the University of Salento with IIT. During the PhD, he was scholar research at the University of South Florida. The aim of his research is the development and application of a new class of polymeric flexible acoustic-based devices.

Francesco Rizzi is currently research staff in the Center of Biomolecular Nanotechnologies of Istituto Italiano di Tecnologia (IIT) in Lecce, Italy. He got a PhD in Physics in 2004. He did his post-doc at Department of Physics and Institute of Photonics, University of Strathclyde, Glasgow (UK), where he won an Experienced Researcher Marie Curie Fellowship. His research interests and activities are related to bio-inspired micro electro-mechanical systems (MEMS) design and fabrication for applications in wearable biological and environmental sensing. He is author of more than 50 manuscripts on international journals, 2 patents, 2 book chapters.

Venkat R. Bhethanabotla obtained his B.S. from Osmania University in Hyderabad, India, and Ph.D. from Penn State in PA, USA, both in Chemical Engineering. He is a Professor of Chemical & Biomedical Engineering and Director of the Materials Science and Engineering Program at University of South Florida. He is a Fellow of the American Institute of Chemical Engineers (AIChE), the American Institute for Medical and Biological Engineering (AIMBE) and the American Association for the Advancement of Science (AAAS). Venkat serves as an associate editor for the IEEE Sensors Journal.

Massimo De Vittorio is Director of the Center for Biomolecular Nanotechnologies of the Istituto Italiano di Tecnologia and Full Professor at Università del Salento (Lecce – Italy). His research activity deals with the development of science and technology applied to nanophotonics and MEMS for applications in life-science and energy. Author of about 330 manuscripts on international journals, 14 patents, he is also senior editor of the Journal IEEE Transactions on Nanotechnology, board member of the international micro and nanoengineering society (iMNEs), member of the editorial board of the Journal Microelectronic Engineering (Elsevier), member of the IEEE EDS Nanotechnology committee.